Magnetic vortex lattice in HgBa$_2$CuO$_{4+\delta}$ observed by small-angle neutron scattering

Yuan Li,[1,2,*] N. Egetenmeyer,[3] J. L. Gavilano,[3] N. Barišić,[4,†] and M. Greven[5]

[1]*Department of Physics, Stanford University, Stanford, California 94305, USA*
[2]*Max Planck Institute for Solid State Research, D-70569 Stuttgart, Germany*
[3]*Laboratory for Neutron Scattering, ETH Zurich and Paul Scherrer Institute, CH-5232 Villigen, Switzerland*
[4]*Physikalisches Institut, Universität Stuttgart, D-70550 Stuttgart, Germany*
[5]*School of Physics and Astronomy, University of Minnesota, Minneapolis, Minnesota 55455, USA*

We report the direct observation of the magnetic vortex lattice in the model high-temperature superconductor HgBa$_2$CuO$_{4+\delta}$. Using small-angle neutron scattering on high-quality crystals, we observe two equal domains of undistorted triangular vortex lattices well aligned with the tetragonal crystallographic axes. The signal decreases rapidly with increasing magnetic field and vanishes above 0.4 T, which we attribute to a crossover from a three-dimensional to a two-dimensional vortex system, similar to previous results for the more anisotropic compound Bi$_{2.15}$Sr$_{1.95}$CaCu$_2$O$_{8+\delta}$. Our result indicates that a triangular vortex lattice (with or without distortion) at low magnetic fields is a generic property of cuprates with critical temperatures above 80 K.

PACS number(s): 74.25.Uv, 61.05.fg, 74.72.Gh

I. INTRODUCTION

The cuprate high-temperature superconductors exhibit a rich variety of mesoscopic phenomena associated with magnetic vortices in the mixed state.[1] In clean samples, the vortices lower their energy by forming a long-range-ordered vortex lattice (VL), which provides an opportunity to study the superconductivity of the bulk. In a simplified picture,[2] the vortex physics is determined by two parameters: the penetration depth λ of magnetic field into the superconducting phase and the coherence length ξ of the superconducting order parameter. Since both of these parameters exhibit pronounced anisotropies in the cuprates, the VL is expected to reflect important characteristics of the superconductivity, such as the d-wave pairing symmetry.[3–6] However, there exists a substantial variation of VL properties among different compounds, including Bi$_{2.15}$Sr$_{1.95}$CaCu$_2$O$_{8+\delta}$ (Bi2212),[7] YBa$_2$Cu$_3$O$_{6+\delta}$ (YBCO),[8,9] and La$_{2-x}$Sr$_x$CuO$_4$ (LSCO).[10] The situation is further complicated by the presence of twin domains and boundaries in the most studied compound, YBCO.[11–13] It is therefore highly desirable to measure a structurally simple representative system to distinguish the generic vortex physics from material-specific aspects.

We report here the direct observation of the VL in HgBa$_2$CuO$_{4+\delta}$ (Hg1201) using small-angle neutron scattering (SANS). Hg1201 is in many ways a model system.[14,15] First, this compound exhibits the highest superconducting critical temperature (T_c) among all cuprates with a single CuO$_2$ layer per primitive unit cell. Notably, our samples exhibit the highest T_c among all materials in which VL studies by SANS have been reported to date. Second, in Hg1201, disorder resides in the Hg-O layer, relatively far away from the CuO$_2$ layer.[16–18] As disorder and defects are common causes for vortex pinning, their relative absence in Hg1201 results in weak pinning[15] and is important for the formation of the VL. Third, Hg1201 features a high tetragonal structural symmetry, and the absence of long-range structural distortions[19] allows us to avoid complications due to vortex pinning at crystallographic twin boundaries. Finally, Hg1201 bridges some differences between other cuprates: LSCO possesses a single-layer structure and relatively low T_c, whereas YBCO and Bi2212 are double-layer compounds with a high T_c. In contrast, Hg1201 possesses a high T_c and it is a single-layer compound.

II. EXPERIMENTAL METHODS

High-quality Hg1201 crystals have recently become available and proven to be suitable for neutron scattering measurements.[20–22] The current study was carried out on two arrays (total mass, approximately 60 and 90 mg) of nearly optimally doped Hg1201 crystals. The crystals were grown by a self-flux method[23] and subsequently heat-treated[15] for up to 180 days to reach the desired homogeneous hole concentration. They were further selected according to the results of magnetometery measurements to ensure high quality[15] and had a uniform T_c of 94 K (determined from the transition midpoint), with a transition width of less than 2 K. The crystals were coaligned and glued on a silicon wafer using an x-ray Laue diffractometer. The c axes of the crystals were within 1° perpendicular to the surface of the wafer, and the a and b axes were coaligned to within 1.5°. Since the two samples gave essentially the same result, we do not distinguish between them in the remainder of this paper. The measurements were performed on the SANS-I spectrometer at the Paul Scherrer Institute, Switzerland. Incident neutrons of wavelengths (λ_n) of 5–10 Å were selected and collimated over a distance of 8–18 m before the sample. Diffracted neutrons were observed by a two-dimensional multidetector located 13–20 m after the sample. The sample was mounted in a horizontal cryomagnet, with the a axis vertical and the c axis pointing along the direction of the applied magnetic field (within 1°). The VL was prepared by cooling the sample from above T_c in a field that was chosen to oscillate about the target value (by ∼1% of the target value). This method[9] improved the VL ordering by keeping the vortices away from local pinning potentials. After reaching the lowest temperature of 2 K, the field was held stationary during the diffraction measurements, which involved rotating the sample and cryomagnet together to angles that brought various diffraction peaks onto the Bragg condition at the detector. Measurements at temperatures between 2 K and

T_c were performed upon heating without changing the field. For all the data presented here, the background measured at $T = 2$ K in zero field or at $T > T_c$ in a field was subtracted from the field-cooled measurements to extract the VL signal.

III. RESULTS

Figure 1 shows diffraction patterns collected at $T = 2$ K for two magnetic fields, $B = 0.2$ and 0.3 T. Data are averaged over multiple sample rotation angles to display all first-order diffraction peaks. Given the tetragonal crystallographic symmetry of Hg1201, the VL is expected to form two equally populated domains aligned with the a and b axes. The presence of 12 (2×6) diffraction peaks with comparable intensities confirms this, and it indicates that the VL is triangular. Well-defined peaks are observed in rocking scans by rotating the sample-magnet assembly, which suggests that the magnetic flux lines are straight and parallel to the c axis.

The radial intensity distribution of the VL signal is displayed in Fig. 2(a). Two spectrometer configurations were used to maximize the signal-to-background ratio at different fields: collimation of 18 m with $\lambda_n = 10$ Å (configuration I) and collimation of 11 m with $\lambda_n = 8$ Å (configuration II). The sample-to-detector distance was equal to 20 m in both cases. The characteristic wave vector magnitude q of the VL is extracted by fitting the data to a Gaussian peak. This quantity is related to the magnetic field through the relation $\sigma = (2\pi/q)^2 B/\Phi_0$, where Φ_0 is the flux quantum $h/2e$, and σ is a geometric factor equal to $\sqrt{3}/2$ or 1 for a triangular or square VL, respectively. As shown in Fig. 2(b), the measured values of σ are consistent with a triangular VL up to $B \approx 0.35$ T. The determination of q using configuration II has somewhat large errors because of the relatively poor momentum resolution. The geometry of the VL can also be determined from the azimuthal intensity distribution near the characteristic value of q. For $B = 0.2$ and 0.25 T, the nearest
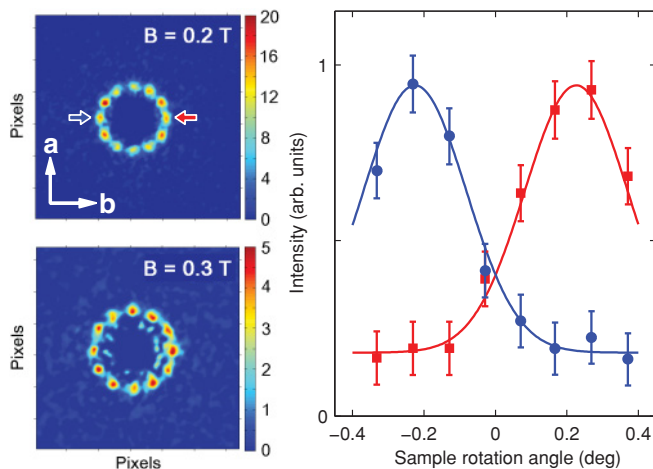
FIG. 1. (Color online) Left: Neutron diffraction patterns at $B = 0.2$ and 0.3 T and $T = 2$ K, averaged over different sample rotation angles. Right: Rocking scans for two Bragg reflections (indicated by the arrows on the left), measured by rotating the sample-magnet assembly with respect to the incident neutron beam.
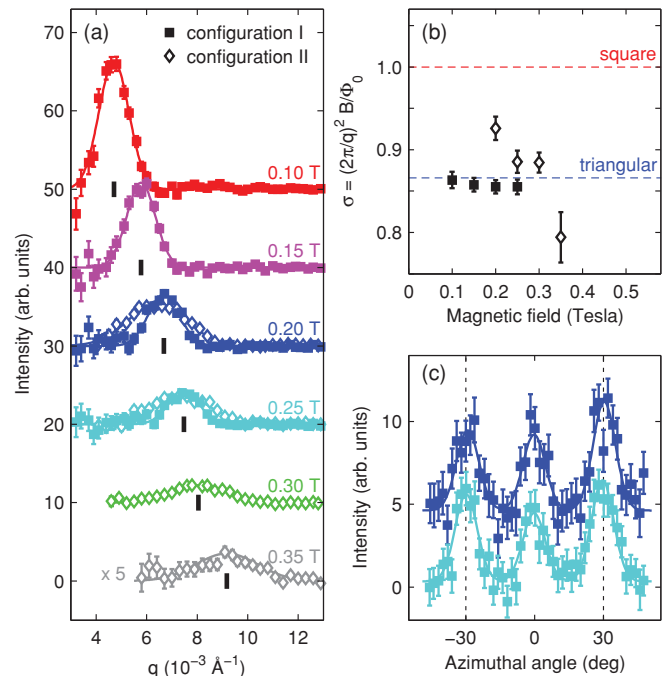
FIG. 2. (Color online) (a) Azimuthally averaged signal amplitudes as a function of momentum transfer q, measured at $T = 2$ K in different magnetic fields. Data obtained with two configurations (see text) are rescaled to allow for a common vertical axis. The $B = 0.35$ T data are, furthermore, multiplied by a factor of 5 for clarity. Vertical bars indicate the fitted value of the characteristic q. (b) VL-structure-dependent coefficient σ (see text) at different fields. Filled and open symbols correspond to configurations I and II, respectively. (c) Azimuthal-angle dependence of the signal measured in configuration I at $T = 2$ K for $B = 0.2$ and 0.25 T. Data in (a) and (c) are vertically offset for clarity.

diffraction peaks from the same type of domain are precisely $60°$ apart [Fig. 2(c)], which is evidence that the triangular VL is undistorted. The fact that no intensity is observed between the peaks indicates that the VL domains are nearly fully aligned with the crystallographic axes.

While it can be seen from Fig. 2(a) that the signal decreases rapidly with increasing magnetic field, the azimuthally averaged intensity does not provide the most accurate determination of the signal amplitude, because the Bragg conditions for different diffraction spots are not simultaneously satisfied. To determine the field dependence of the signal, we employed a procedure that is illustrated in Fig. 3(b): for each of the several magnetic fields measured in a given configuration, a scan is performed on the tilt angle of the sample-magnet assembly, which can be viewed as rotating the Ewald sphere about the Γ point with respect to the two-dimensional reciprocal plane of the VL. The intersection between the Ewald sphere and the two-dimensional reciprocal plane forms a circle that expands as the tilt angle increases [Fig. 3(b)]. When this circle goes through a diffraction spot, the intensity of that spot is maximized, and the different spots have their intensities maximized at different tilt angles [Fig. 3(a)]. To quantify the signal amplitude of the VL, we take the average of the maximal intensities of the five spots on the half of the reciprocal plane that corresponds to the tilting direction [e.g., the average value
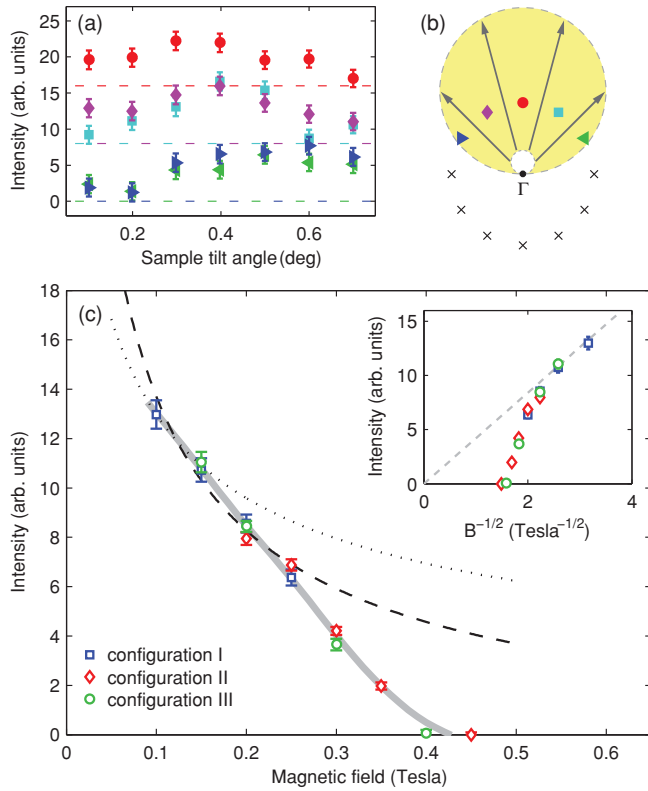
FIG. 3. (Color online) (a) Intensities measured at $T = 2$ K and $B = 0.25$ T in sector boxes surrounding the diffraction peaks indicated by corresponding symbols in (b). The data are offset for clarity, and the same offset is used for reflections that are symmetric about the vertical plane. (b) Illustration of a tilt scan (see text). Broken circles are the intersections of the Ewald sphere with the two-dimensional reciprocal plane at the end points of the scan. Potential diffraction spots are marked by crosses. The five diffraction spots marked by symbols have their Bragg conditions satisfied within the range of the scan. (c) VL intensity measured at $T = 2$ K as a function of magnetic field. Measurements in different configurations are normalized to the values at common magnetic fields. The dotted line is the expected field dependence in the London limit (Eq. (2)); the dashed line is the expected behavior after vortex-core correction (see text), using $B_{c2} = 100$ T (Ref. 24) and the phenomenological parameter $s = 7$; the solid line is a smoothing curve describing the data. The inset shows the same data plotted versus $B^{-1/2}$, where the field dependence expected in the London limit is represented by the dashed line.

of the five maxima in Fig. 3(a) for $B = 0.25$ T]. In addition to configurations I and II, a third configuration, III (collimation of 18 m with $\lambda_n = 8$ Å and a sample-to-detector distance of 18 m) was used as a consistency check, and very good agreement is found among the data sets obtained in different configurations. The result is summarized in Fig. 3(c).

The intensity I_{hk} of VL reflection (h,k) is given by[25]

$$I_{hk} = 2\pi\phi \left(\frac{\mu}{4}\right)^2 \frac{V\lambda_n^2}{\Phi_0^2 q_{hk}} |F_{hk}|^2 \propto \frac{|F_{hk}|^2}{q_{hk}}, \tag{1}$$

where ϕ is the incident neutron flux, μ is the neutron magnetic moment, V is the sample volume, and q_{hk} is the magnitude of the wave vector of the reflection. F_{hk} is the form factor, which is a Fourier component of the spatial variation of the magnetic

field within the VL unit cell. In the London limit (i.e., without considering the effect of vortex cores), F_{hk} is related to the penetration depth λ by

$$F_{hk} = \frac{B}{1 + (q_{hk}\lambda)^2}. \tag{2}$$

For $B \gg B_{c1}$ (the lower critical field), the second term in the denominator is dominant, and this gives $I_{hk} \propto 1/q_{hk} \propto B^{-1/2}$ (since for a given VL symmetry, $q_{hk} \propto \sqrt{B}$). In type II superconductors, the presence of the normal-state vortex cores further reduces the VL signal at high fields,[26] an effect that can be approximated by multiplying Eq. (2) with the correction factor $e^{-s \cdot B/B_{c2}}$, where s is a phenomenological parameter of the order of unity and B_{c2} is the upper critical field. As shown in Fig. 3(c), the measured intensity decreases with increasing field more rapidly than $\propto B^{-1/2}$ above $B \approx 0.15$ T (inset), and more rapidly than the estimated behavior after vortex-core correction above 0.25 T. The signal becomes undiscernibly small above 0.35 T, and measurements at higher fields (up to 4.0 T) do not indicate a reappearance of the signal (not shown).

The disappearance of the VL signal near $B = 0.4$ T can be explained by a mechanism[7] that was first proposed for Bi2212: in an anisotropic superconductor, magnetic vortices are pinned over a characteristic length along the c axis that is related to both the field strength and the anisotropy of the penetration depth, $\gamma \equiv (\lambda_c/\lambda_{ab})$. At sufficiently high fields, this length decreases below the distance between the adjacent CuO$_2$ layers, and the VL decomposes into "vortex pancakes" that are two-dimensionally ordered in each CuO$_2$ layers but are uncorrelated along the c axis. This substantially reduces the spatial variation of the magnetic field and suppresses the diffraction signal. Such a dimensional crossover is expected to occur at $B_{2D} \sim \Phi_0/(\gamma c)^2 \sim 1.4$ T for Hg1201, where $c = 9.6$ Å is the c-axis lattice constant and γ is ~ 40.[27] Both the estimated value of B_{2D} and the measured value of 0.4 T are substantially lower than $B_{c2} = 100$ T[24] and than the magnetic field ($B = 10.8$ T) up to which the VL has been observed in the more isotropic compound YBCO,[9] for which B_{2D} is expected to be much larger than in Hg1201. The difference between the estimated and the measured values of B_{2D} might arise because γ only serves as a phenomenological parameter in determining B_{2D}, and because there is considerable uncertainty in the measured value of γ associated with doping[27] and the experimental method.[24,27–29] We note that the width of the rocking curves in our measurement (Fig. 1) suggests that the magnetic flux lines are straight over long distances. This finding is similar to the case of Bi2212[7] and can be reconciled with the dimensional-crossover mechanism for the VL decomposition if the flux lines are distorted only over short distances. In other words, as the flux lines break down into vortex pancakes, the magnetic field profile projected onto the basel plane dramatically loses its contrast, but the correlation between the averaged location of the flux lines (or stacks of vortex pancakes) remains intact. Finally, for the vortex pancakes that belong to a single flux line to be misaligned along the c axis, the pancakes in different CuO$_2$ layers do not need to be individually pinned; instead, neighboring pancakes in the same CuO$_2$ layer may be effectively pinned together
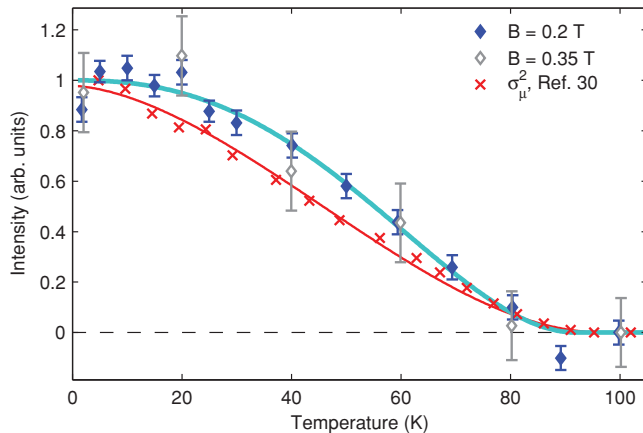
FIG. 4. (Color online) Temperature dependence of diffraction intensity measured at two different magnetic fields compared with a μSR result for optimally-doped Hg1201.[30] The value at $T = 100$ K is set to zero, and the data are normalized to the values at low temperature. The solid lines are empirical fits as guides to the eye (see text).

if the 2D correlation length of the VL is larger than the size of each pancake and than the characteristic distance between neighboring pinning centers in the same layer. Given the well-defined diffraction patterns in Figs. 1 and 2(c), it is likely that the vortex pancakes are pinned in this fashion by a low density of pinning centers.

The temperature dependence of the VL signal was measured in two magnetic fields, $B = 0.2$ and 0.35 T. For each field, the measurement was performed at a fixed sample angle, and the intensities of multiple diffraction peaks were summed together to improve the counting statistics. Apart from a rescaling factor for the overall intensity, the temperature dependence measured in the two fields is identical (Fig. 4). Since $B = 0.35$ T is very close to the field at which the VL signal vanishes, this suggests that the decrease in signal as T_c is approached (due to the increasing penetration depth: $I \propto \lambda^{-4}$) and the disappearance of the signal at $T = 2$ K above $B = 0.4$ T have different causes. The similarity of the temperature dependences in the two fields further supports the dimensional-crossover scenario of the VL decomposition, since B_{2D} is related to the anisotropy γ, which is nearly independent of temperature.[24]

The data in Fig. 4 can be described by the empirical function $I \propto [1 - (T/T_c)^\alpha]^2$. The fitted value for T_c is 92 ± 5 K, consistent with the T_c value determined by magnetic susceptibility measurements (94 ± 1 K). The fitted value $\alpha = 2.4 \pm 0.3$ is rather different from that of the "two-fluid" empirical expression ($\alpha = 4$) for conventional superconductors, which seems to describe early muon-spin-rotation (μSR) results for YBCO.[31] (In μSR experiments, the measured muon relaxation rate σ_μ is proportional to λ^{-2}, and therefore σ_μ^2 is expected to be proportional to the signal amplitude measured by SANS.) Our result is also somewhat different from the more recent μSR result for Hg1201,[30] which is included in Fig. 4 and for which σ_μ^2 can be described by the same function with $\alpha = 1.6$. These differences need to be further understood. We note that a discrepancy between SANS and μSR results regarding the temperature dependence has been

documented previously,[32] and the temperature dependence that we observe is consistent with other SANS measurements in cuprates.[7,32] For *d*-wave superconductors like the cuprates, a more quantitative description of the data near $T = 0$ K may require a correction to account for nonlocal effects.[33]

IV. DISCUSSION AND CONCLUSION

Now we discuss the implication of our results for the VL physics of the cuprates. So far, well-defined VLs at $B > 1$ T have been observed only in YBCO and LSCO,[8–10] and the results are drastically different: in YBCO,[9] a (distorted) triangular VL pattern is observed at low fields, and a square pattern is observed only at $B > 6.7$ T, with the nearest-neighbor direction along the Cu-Cu diagonal of the unit cell. In contrast, a square pattern is already well developed at $B = 0.4$ T in LSCO,[10] and the nearest-neighbor direction is along the Cu-O bond, 45° from that in YBCO. A square VL has also been observed in the electron-doped cuprate $Nd_{2-x}Ce_xCuO_4$ (NCCO)[34] down to $B = 0.05$ T. Our result for Hg1201 indicates that a unified picture may still exist for cuprates with high values of T_c (>80 K), in which a triangular VL is favored at low fields ($B < 0.5$ T). We note that a nearly undistorted triangular VL was recently also observed in the iron-based superconductor KFe_2As_2 ($T_c = 3.6$ K) up to $B = 0.9$ T,[35] which further supports the notion that a triangular VL is favored at low fields. The low triangular-to-square VL transition fields in LSCO and NCCO may empirically be related to their relatively low T_c values compared to those of YBCO and Hg1201 and/or to the former compounds' common body-centered crystal structure (the latter have a non-body-centered structure). Recently, it was suggested[36] that a universal VL phase diagram featuring a first-order transition with increasing field from a triangular to a square VL may be expected in tetragonal (or weakly orthorhombic, such as YBCO) systems as a result of the anisotropies of the Fermi velocity and the superconducting gap. To test this theoretical proposal further, measurements of the VL in Hg1201 and Bi2212 at higher fields (especially using local probes) are desirable.

In conclusion, we have used SANS to observe the VL in Hg1201 near optimal doping. Our data suggest that a triangular VL at low fields ($B < 0.5$ T) is generic to cuprates with high T_c and a non-body-centered structure. The difficulty in using SANS to measure VLs at high fields in Hg1201 is likely the result of a decomposition of magnetic flux lines into 2D vortex pancakes. This prevents us from further investigating the anisotropic properties of Hg1201, and future studies of the VL using local magnetic probes are desirable.

*Corresponding author: yuan.li@fkf.mpg.de

†Present address: School of Physics and Astronomy, University of Minnesota, Minneapolis, Minnesota 55455, USA.

[1] G. Blatter, M. V. Feigel'man, V. B. Geshkenbein, A. I. Larkin, and V. M. Vinokur, Rev. Mod. Phys. **66**, 1125 (1994).

[2] A. A. Abrikosov, Sov. Phys. JETP **5**, 1174 (1957).

[3] I. Affleck, M. Franz, and M. H. S. Amin, Phys. Rev. B **55**, R704 (1997).

[4] M. Ichioka, N. Enomoto, and K. Machida, J. Phys. Soc. Jpn. **66**, 3928 (1997).

[5] M. Ichioka, A. Hasegawa, and K. Machida, Phys. Rev. B **59**, 8902 (1999).

[6] J. Shiraishi, M. Kohmoto, and K. Maki, Phys. Rev. B **59**, 4497 (1999).

[7] R. Cubitt, E. M. Forgan, G. Yang, S. L. Lee, D. Paul, H. A. Mook, M. Yathiraj, P. H. Kes, T. Li, A. A. Menovsky, Z. Tarnawski, and K. Mortensen, Nature (London) **365**, 407 (1993).

[8] S. P. Brown, D. Charalambous, E. C. Jones, E. M. Forgan, P. G. Kealey, A. Erb, and J. Kohlbrecher, Phys. Rev. Lett. **92**, 067004 (2004).

[9] J. S. White, V. Hinkov, R. W. Heslop, R. J. Lycett, E. M. Forgan, C. Bowell, S. Strässle, A. B. Abrahamsen, M. Laver, C. D. Dewhurst, J. Kohlbrecher, J. L. Gavilano, J. Mesot, B. Keimer, and A. Erb, Phys. Rev. Lett. **102**, 097001 (2009).

[10] R. Gilardi, J. Mesot, A. Drew, U. Divakar, S. L. Lee, E. M. Forgan, O. Zaharko, K. Conder, V. K. Aswal, C. D. Dewhurst, R. Cubitt, N. Momono, and M. Oda, Phys. Rev. Lett. **88**, 217003 (2002).

[11] M. Yethiraj, H. A. Mook, G. D. Wignall, R. Cubitt, E. M. Forgan, D. M. Paul, and T. Armstrong, Phys. Rev. Lett. **70**, 857 (1993).

[12] B. Keimer, F. Dogbrevean, I. A. Aksay, R. W. Erwin, J. W. Lynn, and M. Sarikaya, Science **262**, 83 (1993).

[13] S. T. Johnson, E. M. Forgan, S. H. Lloyd, C. M. Aegerter, S. L. Lee, R. Cubitt, P. G. Kealey, C. Ager, S. Tajima, A. Rykov, and D. McK. Paul, Phys. Rev. Lett. **82**, 2792 (1999).

[14] H. Eisaki, N. Kaneko, D. L. Feng, A. Damascelli, P. K. Mang, K. M. Shen, Z.-X. Shen, and M. Greven, Phys. Rev. B **69**, 064512 (2004).

[15] N. Barišić, Y. Li, X. Zhao, Y.-C. Cho, G. Chabot-Couture, G. Yu, and M. Greven, Phys. Rev. B **78**, 054518 (2008).

[16] J. Wagner, P. Radaelli, D. Hinks, J. Jorgensen, J. Mitchell, B. Dabrowski, G. Knapp, and M. Beno, Physica C **210**, 447 (1993).

[17] D. Pelloquin, V. Hardy, A. Maignan, and B. Raveau, Physica C **273**, 205 (1997).

[18] V. Viallet, A. Bertinotti, J.-F. Marucco, D. Colson, L. Fruchter, G. L. Bras, V. Vulcanescu, and J. Hammann, Physica C **282-287**, 1073 (1997).

[19] A. M. Balagurov, D. V. Sheptyakov, V. L. Aksenov, E. V. Antipov, S. N. Putilin, P. G. Radaelli, and M. Marezio, Phys. Rev. B **59**, 7209 (1999).

[20] Y. Li, V. Balédent, N. Barišić, Y. Cho, B. Fauqué, Y. Sidis, G. Yu, X. Zhao, P. Bourges, and M. Greven, Nature (London) **455**, 372 (2008).

[21] G. Yu, Y. Li, E. M. Motoyama, X. Zhao, N. Barišić, Y. Cho, P. Bourges, K. Hradil, R. A. Mole, and M. Greven, Phys. Rev. B **81**, 064518 (2010).

[22] Y. Li, V. Balédent, G. Yu, N. Barišić, K. Hradil, R. A. Mole, Y. Sidis, P. Steffens, X. Zhao, P. Bourges, and M. Greven, Nature (London) **468**, 283 (2010).

[23] X. Zhao, G. Yu, Y.-C. Cho, G. Chabot-Couture, N. Barišić, P. Bourges, N. Kaneko, Y. Li, L. Lu, E. M. Motoyama, O. P. Vajk, and M. Greven, Adv. Mater. **18**, 3243 (2006).

[24] G. L. Bras, L. Fruchter, V. Vulcanescu, V. Viallet, A. Bertinotti, A. Forget, J. Hammann, J. F. Marucco, and D. Colson, Physica C **271**, 205 (1996).

[25] D. K. Christen, F. Tasset, S. Spooner, and H. A. Mook, Phys. Rev. B **15**, 4506 (1977).

[26] A. Yaouanc, P. Dalmas de Réotier, and E. H. Brandt, Phys. Rev. B **55**, 11107 (1997).

[27] C. Panagopoulos, T. Xiang, W. Anukool, J. R. Cooper, Y. S. Wang, and C. W. Chu, Phys. Rev. B **67**, 220502 (2003).

[28] C. Panagopoulos, J. R. Cooper, T. Xiang, G. B. Peacock, I. Gameson, and P. P. Edwards, Phys. Rev. Lett. **79**, 2320 (1997).

[29] G. D. Gu, R. Puzniak, K. Nakao, G. J. Russell, and N. Koshizuka, Supercond. Sci. Technol. **11**, 1115 (1998).

[30] B. Nachumi, A. Keren, K. Kojima, M. Larkin, G. M. Luke, J. Merrin, W. D. Wu, Y. J. Uemura, Y. Xue, F. Chen, Q. Xiong, Z. Huang, Z. He, Q. Lin, J. Clayhold, and C. W. Chu, Hyperfine Interact. **105**, 119 (1997).

[31] D. R. Harshman, L. F. Schneemeyer, J. V. Waszczak, G. Aeppli, R. J. Cava, B. Batlogg, L. W. Rupp, E. J. Ansaldo, and D. L. Williams, Phys. Rev. B **39**, 851 (1989).

[32] E. M. Forgan, D. M. Paul, H. A. Mook, P. A. Timmins, H. Keller, S. Sutton, and J. S. Abell, Nature (London) **343**, 735 (1990).

[33] I. Kosztin and A. J. Leggett, Phys. Rev. Lett. **79**, 135 (1997).

[34] R. Gilardi, J. Mesot, S. P. Brown, E. M. Forgan, A. Drew, S. L. Lee, R. Cubitt, C. D. Dewhurst, T. Uefuji, and K. Yamada, Phys. Rev. Lett. **93**, 217001 (2004).

[35] H. Kawano-Furukawa, C. J. Bowell, J. S. White, R. W. Heslop, A. S. Cameron, E. M. Forgan, K. Kihou, C. H. Lee, A. Iyo, H. Eisaki, T. Saito, H. Fukazawa, Y. Kohori, R. Cubitt, C. D. Dewhurst, J. L. Gavilano, and M. Zolliker, e-print: arXiv:1005.4468v2.

[36] K. M. Suzuki, K. Inoue, P. Miranović, M. Ichioka, and K. Machida, J. Phys. Soc. Jpn. **79**, 013702 (2010).